Structural Engineering and Mechanics, Vol. 7, No. 5 (1999) 457-471
DOI: http://dx.doi.org/10.12989/sem.1999.7.5.457

Viscoplastic analysis of thin-walled tubes under cyclic bending

Wen-Fung Pan†

Department of Engineering Science, National Cheng Kung University, Tainan, Taiwan 701, R.O.C.

Chien-Min Hsu‡

Department of Arts-Craft, Tung Fung Junior College of Technology, Kao Hsiung County, Taiwan, R.O.C.

Abstract. In this paper, different curvature-rates are controlled to highlight the characteristic of viscoplastic response in cyclic bending tests. The curvature-ovalization apparatus, which was designed by Pan *et al.* (1998), is used for conducting the curvature-controlled experiments on thin-walled tubular specimens for AISI 304 stainless steel under cyclic bending. The results reveals that the faster the curvature-rate implies, the fast degree of hardening of the metal tube. However, the ovalization of the tube cross-section increases when the curvature-rate increases.

Key words: viscoplastic response; thin-walled tube; cyclic bending; endochronic theory.

1. Introduction

The thin-walled tube components in a number of practical industrial applications, such as offshore structures, nuclear reactor components, earthquake resistant structures, ..etc., must be designed to resist cyclic bending. It is well known that the ovalization of the tube cross-section (Brazier effect 1927) is observed when a thin-walled tube is subjected to bending. If the bending moment increases, the magnitude of the ovalization also increased (Brazier 1927, Reissner and Weinitschke 1963, Reddy 1979, Kyrikides and Shaw 1982). If a thin-walled tube is subjected to cyclic bending, the magnitude of the ovalization increases with the number of cycles (Shaw and Kyriakides 1985, Kyriakides and Shaw 1987). Increase in ovalization of the tube cross-section causes a progressive reduction in the bending rigidity (accumulation of damage) which can result in buckling or fracture of the tube component (Gellin 1980, Fabian 1981, Corona and Kyriakides 1987, Corona and Kyriakides 1988, Kyriakides and Ju 1992). Therefore, the study of the mechanical behaviors of the thin-walled tube subjected to cyclic bending is of importance in many industrial applications.

Previous experimental investigations have demonstrated that engineering alloys such as 304 and 316 stainless steels, high-strength titanium alloys, exhibit viscoplastic behavior (Krempl 1979,

† Professor
‡ Instructor

Kujawski and Krempl 1981, Ikegami and Ni-Itsu 1983). Therefore, once the thin-walled tube, which is fabricated by the aforementioned metals, is manipulated under pure bending or cyclic bending with different loading-rates, the response of the tube for each loading-rate is expected to generate differently. Based on this point of view, the following experimental and theoretical studies on the mechanical behaviors of the thin-walled tubes subjected to cyclic bending at different controlled curvature-rates are discussed in this paper.

For experimental aspect, a four-point cyclic bending machine (similar to the facilities reported in Kyriakides and Shaw 1982, Shaw and Kyriakides 1985, Corona and Kyriakides 1988) is used for conducting the cyclic bending test. The material of the thin-walled tube chosen for experimental study is AISI 304 stainless steel. The curvature-rates in this test are 2×10^{-1} and 2×10^{-3} m^{-1}/sec, which are the maximum and minimum curvature-rates controlled by the bending machine. To avoid any end effect caused by the bending machine, the curvature is controlled and measured by a curvature-ovalization measurement apparatus (COMA), which was designed by Pan *et al.* (1998). The ovalization of the tube cross-section is also measured by the COMA. The magnitude of the bending moment is obtained from the two load cells which are mounted in the bending machine. It is found that from the moment-curvature and ovalization-curvature curves of the thin-walled tube under cyclic bending at different curvature-rates that the material hardens when curvature-rate increases, and the ovalization of the tube cross-section also increases with the number of cycles.

For theoretical aspect, we employ the first-order ordinary differential constitutive equations of the theory obtained by Murakami and Read (1989) with the rate-sensitivity function proposed by Pan and Chern (1997) to investigate the viscoplastic responses of thin-walled tube subjected to cyclic bending. The principle of virtual work is used to formulate the problem, which results in a set of nonlinear equations that has to be solved numerically. Thus, the relationship among bending moment, tube curvature and ovalization of the tube cross-section can be determined from the necessary equilibrium equations. It is shown that a satisfactory description by the theory has been achieved by comparing with the experimental data.

2. Experimental facilities

2.1. Bending device

The bending device is schematically shown in Fig. 1. It is designed as a four-point bending machine, capable of applying reverse bending (similar to the facilities reported in references (Shaw and Kyriakides 1985, Kyriakides and Shaw 1987, Kyriakides and Ju 1992)). The device consists of two rotating sprockets resting on two support beams. Heavy chains run around the sprockets and are connected to two hydraulic cylinders and load cells forming a closed loop. Once either the top or bottom cylinder is contracted, the sprockets are rotated, and pure bending of the test specimen is achieved. Reverse bending can be achieved by reversing the direction of flow in the hydraulic circuit. Detailed description of the bending device can be found in several references (Shaw and Kyriakides 1985, Kyriakides and Shaw 1987, Kyriakides and Ju 1992).

The two sprockets rest on two heavy support beams 1.25m apart. This allows a maximum length of the test specimen to be 1m. The bending capacity of the machine is 5300N-m. Each tube is tested and fitted with solid rod extension, as shown in Fig. 2. The contact between tube and the rollers is free to move along axial direction during bending. The load transfer to the test

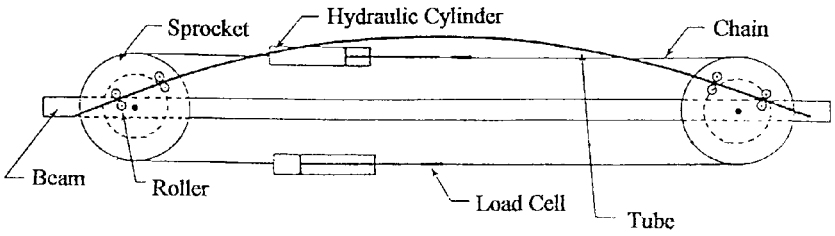

Fig. 1 Cyclic bending testing facilities

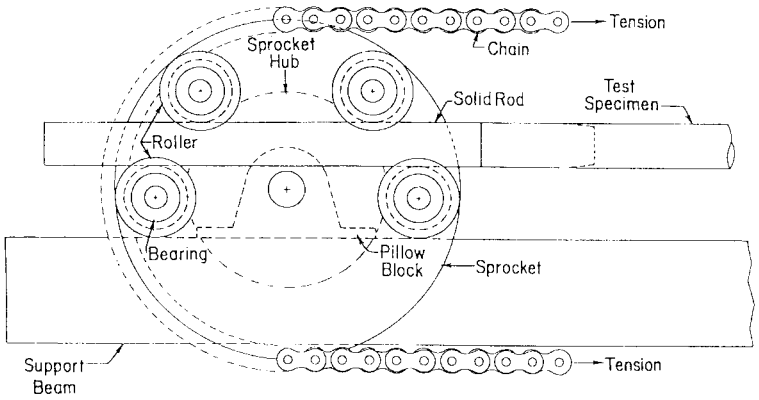

Fig. 2 Load transfer assembly

specimen is in the form of a couple formed by concentrated loads from two of the rollers. The applied bending moment is directly proportional to the tension in the chains. Based on the signal from two load cells, the bending moment M exerted on the tube is calculated as

$$M = FR \tag{1}$$

where F is the force on the chain, which can be obtained from the pressure and area of the cylinder, and R is the radius of the sprocket.

2.2. Curvature-ovalization measurement apparatus (COMA)

The curvature-ovalization measurement apparatus (COMA), which was designed by Pan *et al.* (1998), is lightweight and is mounted close to the tube mid-span (shown in Fig. 3). It can be used to monitor the changes in major and minor diameters of the tube cross-section, using a magnetic detector (middle part of the COMA). Simultaneously, it can be used to measure variations in the tube curvature close to the mid-span from the signals of inclinometers. There are three inclinometers in the COMA. Two of them are fixed on two holders, which are denoted as side-inclinometers 1 and 2, respectively (see Fig. 3). The holders are fixed on the circular tube before the test begins. The angles of rotation detected by these two side-inclinometers are in x-y plane which is the direction of the bending moment (see Fig. 4). To ensure the measurement of these two side-inclinometers in the same plane, a ring with ball bearings is designed which is connected to these two holders by two solid rods. Four railway tracks on the surface of the vertical solid cylinder are used for guiding the movement of the ring. To avoid any deformation of the solid rods, this ring is free to move vertically. The changes in angles of these two side-inclinometers

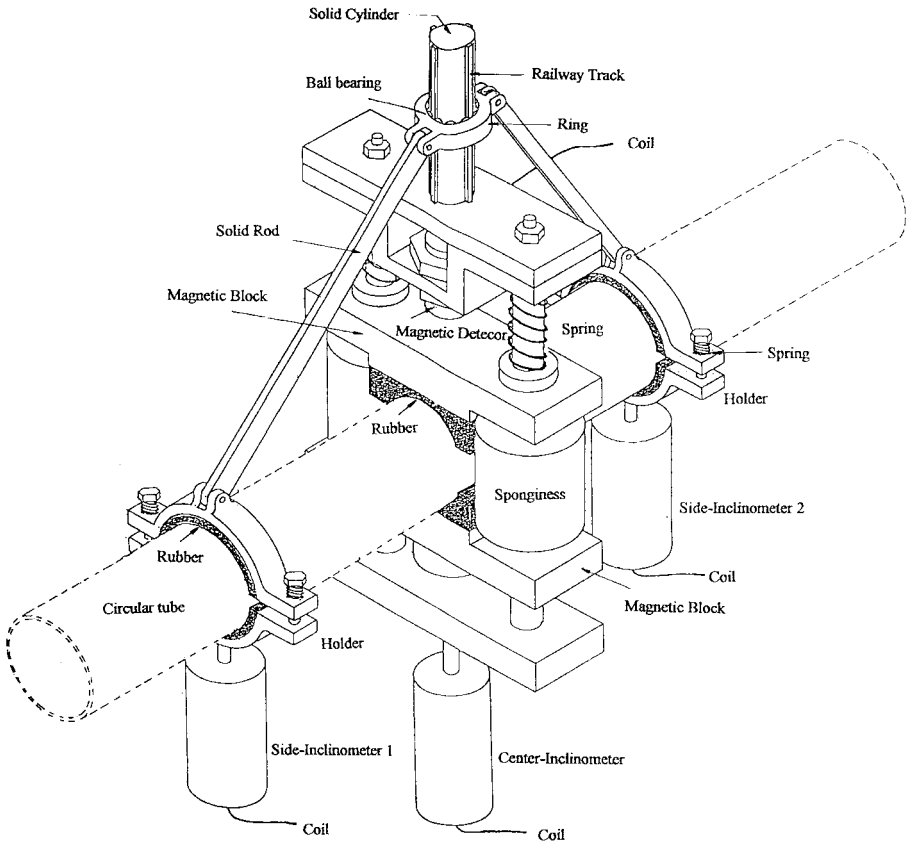

Fig. 3 Curvature-ovalization measurement apparatus (COMA)

can be detected and transferred into tube curvature. An additional inclinometer (denoted as center-inclinometer) is also used, which is fixed at the center part of the COMA, as shown in Fig. 3. The angle of rotation detected by center-inclinometer is in y-z plane, which is perpendicular to the plane of the bending moment (see Fig. 4). The center-inclinometer can be used for inspecting the

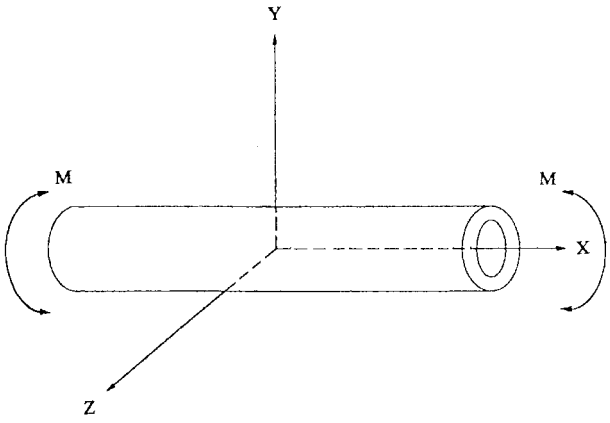

Fig. 4 Coordinate system of the tube specimen under pure bending

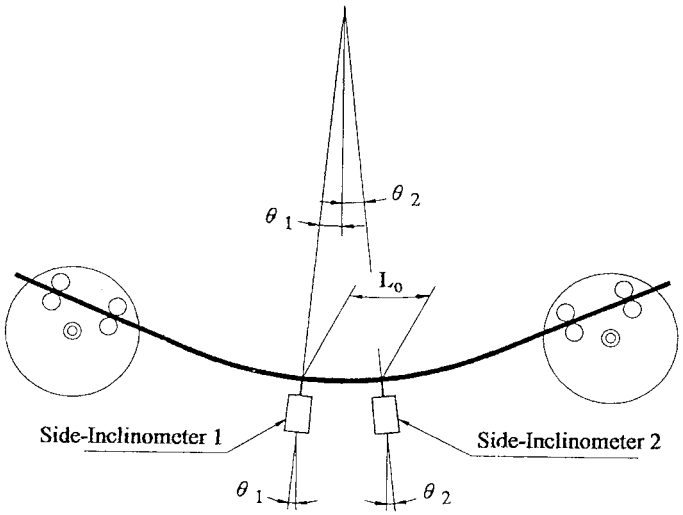

Fig. 5 Angle changes measured by two side-inclinometers under pure bending

deviation of the plane, in which the aforementioned two side-inclinometers are fixed, from the plane of bending moment (x-y plane).

Once the two holders are placed and fixed on the circular tube, the distance between the two side-inclinometers is fixed, which is denoted as L_o. Let us now consider that the circular tube is subjected to pure bending, as shown in Fig. 5. The angle changes detected by the two side-inclinometers are denoted as θ_1 and θ_2. Due to the uniform bending in all sections, the circular tube, which is originally a straight line, is deformed into an arc of circle. The distance between the center of this arc and the neutral surface is denoted as ρ (shown in Fig. 6). From Fig. 6, the value of L_o is determined as

$$L_o = \rho(\theta_1 + \theta_2) \tag{2}$$

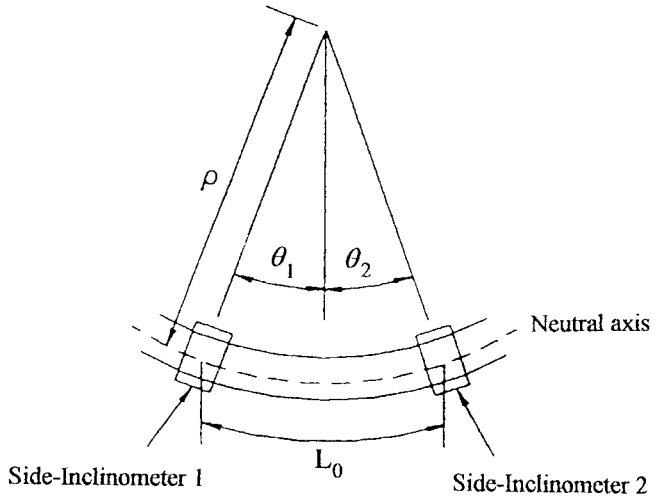

Fig. 6 Longitudinal deformation between two side-inclinometers under pure bending

The curvature of the tube κ is

$$\kappa = \frac{1}{\rho} = \frac{(\theta_1 + \theta_2)}{L_o} \tag{3}$$

It can be seen that the COMA is mounted close to the mid-span of the circular tube, which is far away from the rotating sprockets and inserted solid rods. Therefore, the effects of the sprockets and solid bars are thus relatively small.

3. Problem formulation

In this section, we formulate the problem of response for thin-walled tube subjected to bending. The kinematics of the tube cross section, the constitutive model for viscoplastic response and the principle of virtual work are discussed separately as follows:

3.1. Kinematics

A long, circular, thin-walled tube under combined bending and external pressure is considered in this study. Fig. 7 shows the problem geometry, in which M is the applied moment, κ is the resultant curvature, R is the mean radius, and t is the wall thickness. Based on axial, circumferential and radial coordinates x, θ and z, the displacements of a point of the tube's mid-surface are denoted as u, v and w, respectively. The plane sections are assumed here to be perpendicular to the tube mid-surface before and during bending deformation. In addition, the strains are assumed to remain small; however, finite rotations in both axes under bending are allowed. The circumferential strain of the deformation is expressed as (Kyriakides and Shaw 1982, Shaw and Kyriakides 1985, Kyriakides and Ju 1992):

$$\varepsilon_\theta = \varepsilon_\theta^0 + z\,\kappa_\theta \tag{4}$$

where

$$\varepsilon_\theta^0 = \left(\frac{v' + w}{R}\right) + \frac{1}{2}\left(\frac{v' + w}{R}\right)^2 + \frac{1}{2}\left(\frac{v - w'}{R}\right)^2 \tag{5}$$

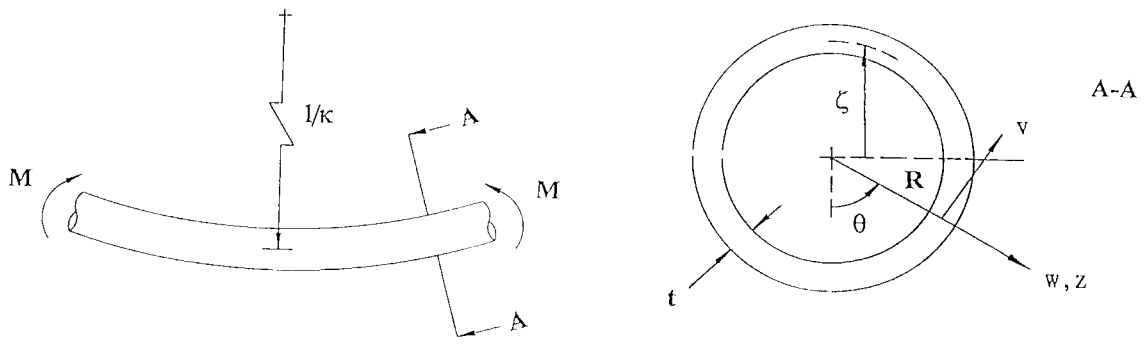

Fig. 7 Problem geometry

and

$$\kappa_\theta = \left(\frac{v' - w''}{R^2}\right) \Big/ \sqrt{1 - \left(\frac{v - w'}{R}\right)^2} \tag{6}$$

The axial strain is expressed as

$$\varepsilon_x = \varepsilon_x^0 + \xi\kappa \tag{7}$$

and

$$\xi = [(R + w)\cos\theta - v\ \sin\theta + z\ \cos\theta] \tag{8}$$

where ε_x^0 is the axial strain of the cylinder's axis. Note that the amount of ε_x^0 is generally not zero due to the shifting of the neutral axis under bending.

3.2. Endochronic constitutive equations

The endochronic theory is adopted for simulating the elasto-plastic response of a long, circular, thin-walled tube under combined bending and external pressure. Owing to the highly nonproportional path of the stress history, the incremental form of endochronic theory should be considered in formulating the problem. According to the condition of small deformation for homogeneous and isotropic materials, the increment of deviatoric stress tensor $d\underset{\sim}{s}$ of endochronic theory is given as (Valanis 1980)

$$d\underset{\sim}{s} = 2\rho(0)\, d\underset{\sim}{e}^p + 2\underset{\sim}{h}(z)\, dz \tag{9}$$

and

$$\underset{\sim}{h}(z) = \int_0^z \frac{d\rho(z - z')}{dz} \frac{\partial \underset{\sim}{e}^p}{\partial z'} dz' \tag{10}$$

where z is the intrinsic time scale, $\rho(z)$ is termed the kernel function and $\underset{\sim}{e}^p$ is the deviatoric plastic strain tensor which is defined as

$$d\underset{\sim}{e}^p = d\underset{\sim}{e} - \frac{d\underset{\sim}{s}}{2\mu_0} \tag{11}$$

where $\underset{\sim}{e}$ denotes the deviatoric strain tensor, and μ_0 is the elastic shear modulus. The intrinsic time measure ζ is

$$d\zeta = k \mid d\underset{\sim}{e}^p \mid \quad \text{or} \quad d\zeta^2 = k^2\, d\underset{\sim}{e}^p \cdot d\underset{\sim}{e}^p \tag{12a,b}$$

in which k is the rate-sensitivity function. The function k for describing the viscoplastic behavior of material subjected to multiaxial loading is expressed as (Pan and Chern 1997)

$$k = 1 - k_a \log\left[\frac{\dot{e}_{eq}^p}{(\dot{e}_{eq}^p)_o}\right] \tag{13}$$

where k_a is a rate-sensitivity parameter, $(\dot{e}_{eq}^p)_o$ is the reference equivalent deviatoric plastic strain-rate, and $\dot{e}_{eq}^p$ is the relative equivalent deviatoric plastic strain-rate. The material function (or hardening function) $f(\zeta)$ is

$$f(\zeta)=\frac{d\zeta}{dz}=1-C\ e^{-\beta\zeta},\quad \text{for}\quad C<1 \tag{14}$$

in which C and β are material parameters. If the plastically incompressible is satisfied, the elastic hydrostatic response can be written as

$$d\sigma_{kk}=3K\ d\varepsilon_{kk} \tag{15}$$

where σ_{kk} and ε_{kk} are the trace of stress and strain tensors, respectively, and K is the elastic bulk modulus. According to the mathematical characteristic of the kernel function $\rho(z)$, Eq. (9) is expressed as (Murakami and Read 1989, Pan *et al.* 1996, Pan and Chern 1997)

$$d\underset{\sim}{s}=\sum_{i=1}^{n} d\underset{\sim}{s}_i=2\sum_{i=1}^{n} C_i\ d\underset{\sim}{e}^{p}-\sum_{i=1}^{n}\alpha_i\ \underset{\sim}{s}_i\ dz \tag{16}$$

where C_i and α_i are material constants. Substituting Eq. (11) into Eq. (16) leads to

$$d\underset{\sim}{s}=\frac{\mu_0}{\mu_0+\sum_{i=1}^{n} C_i}\left[2\sum_{i=1}^{n} C_i\ d\underset{\sim}{e}-\sum_{i=1}^{n}\alpha_i\ \underset{\sim}{s}_i\ dz\right] \tag{17}$$

By using Eq. (15), Eq. (17) can be expressed in terms of the stress and strain tensors as

$$d\underset{\sim}{\sigma}=p_1\ d\underset{\sim}{\varepsilon}+p_2\ d\varepsilon_{kk}\ \underset{\sim}{I}+p_3\sum_{i=1}^{n}\alpha_i\ (\underset{\sim}{\sigma}-\frac{\sigma_{kk}}{3}\underset{\sim}{I})_i\ dz \tag{18}$$

where

$$p_1=\frac{2\sum_{i=1}^{n} C_i}{1+\dfrac{\sum_{i=1}^{n} C_i}{\mu_0}},\quad p_2=K-\frac{2\sum_{i=1}^{n} C_i}{3\left(1+\dfrac{\sum_{i=1}^{n} C_i}{\mu_0}\right)},\quad p_3=\frac{-1}{1+\dfrac{\sum_{i=1}^{n} C_i}{\mu_0}}$$

According to axial, circumferential and radial coordinates x, θ and z, the stress and strain tensors of thin-walled tube for the case of biaxial loading are

$$\underset{\sim}{\sigma}=\begin{bmatrix}\sigma_x & 0 & 0\\ 0 & \sigma_\theta & 0\\ 0 & 0 & 0\end{bmatrix}\qquad \underset{\sim}{\varepsilon}=\begin{bmatrix}\varepsilon_x & 0 & 0\\ 0 & \varepsilon_\theta & 0\\ 0 & 0 & \varepsilon_r\end{bmatrix} \tag{19a,b}$$

The increment of the deviatoric plastic strain tensor $d\underset{\sim}{e}^{p}$ from Eq. (11) is

$$d\underset{\sim}{e}^{p}=\begin{bmatrix}\dfrac{2d\varepsilon_x-d\varepsilon_\theta-d\varepsilon_r}{3}-\dfrac{2d\sigma_x-d\sigma_\theta}{6\mu_0} & 0 & 0\\ 0 & \dfrac{2d\varepsilon_\theta-d\varepsilon_x-d\varepsilon_r}{3}-\dfrac{2d\sigma_\theta-d\sigma_x}{6\mu_0} & 0\\ 0 & 0 & \dfrac{2d\varepsilon_r-d\varepsilon_x-d\varepsilon_\theta}{3}+\dfrac{d\sigma_x+d\sigma_\theta}{6\mu_0}\end{bmatrix} \tag{20}$$

Substitution of Eqs. (19a) and (19b) into Eq. (18) yields

$$d\sigma_x = p_1\, d\varepsilon_x + p_2\,(d\varepsilon_x + d\varepsilon_\theta + d\varepsilon_r) + p_3 \sum_{i=1}^{3} \alpha_i \left(\frac{2\sigma_x - \sigma_\theta}{3} \right)_i dz \tag{21}$$

$$d\sigma_\theta = p_1\, d\varepsilon_\theta + p_2\,(d\varepsilon_x + d\varepsilon_\theta + d\varepsilon_r) + p_3 \sum_{i=1}^{n} \alpha_i \left(\frac{2\sigma_\theta - \sigma_x}{3} \right)_i dz \tag{22}$$

$$0 = p_1\, d\varepsilon_r + p_2\,(d\varepsilon_x + d\varepsilon_\theta + d\varepsilon_r) - p_3 \sum_{i=1}^{n} \alpha_i \left(\frac{\sigma_x - \sigma_\theta}{3} \right)_i dz \tag{23}$$

From Eq. (23), one obtains

$$d\varepsilon_r = A_1\, d\varepsilon_x + A_1\, d\varepsilon_\theta + A_2\, dz \tag{24}$$

where

$$A_1 = \frac{-p_2}{p_1 + p_2}, \quad A_2 = \frac{p_3}{p_1 + p_2} \sum_{i=1}^{n} \alpha_i \left(\frac{\sigma_x + \sigma_\theta}{3} \right)_i \tag{25a,b}$$

Substituting Eq. (24) into Eqs. (21) and (22) leads to

$$d\sigma_x = A_3\, d\varepsilon_x + A_4\, d\varepsilon_\theta + A_5\, dz \tag{26}$$

and

$$d\sigma_\theta = A_4\, d\varepsilon_x + A_3\, d\varepsilon_\theta + A_6\, dz \tag{27}$$

where

$$A_3 = p_1 + p_2 + p_2 A_1$$

$$A_4 = p_2 + p_2 A_1$$

$$A_5 = p_2 A_2 + p_3 \sum_{i=1}^{n} \alpha_i \left(\frac{2\sigma_x - \sigma_\theta}{3} \right)_i$$

$$A_6 = p_2 A_2 + p_3 \sum_{i=1}^{n} \alpha_i \left(\frac{2\sigma_\theta - \sigma_x}{3} \right)_i \tag{28a,b,c,d}$$

By substituting Eqs. (14), (20), (24), (26) and (27) in Eq. (12b), a quadratic form with variable dz is determined to be

$$\frac{f(\zeta)^2 dz^2}{k^2} = (B_1 d\varepsilon_x + B_2 d\varepsilon_\theta + B_3 dz)^2 + (B_2 d\varepsilon_x + B_1 d\varepsilon_\theta + B_4 dz)^2 + (B_5 d\varepsilon_x + B_5 d\varepsilon_\theta + B_6 dz)^2 \tag{29}$$

where

$$B_1 = \frac{2 - A_1}{3} - \frac{2A_3 - A_4}{6\mu_o}$$

$$B_2 = -\frac{1+A_1}{3} - \frac{2A_4 - A_3}{6\mu_o}$$

$$B_3 = -\frac{A_2}{3} + \frac{2A_5 - A_6}{6\mu_o}$$

$$B_4 = -\frac{A_2}{3} - \frac{2A_6 - A_5}{6\mu_o}$$

$$B_5 = \frac{2A_1 - 1}{3} - \frac{A_3 + A_4}{6\mu_o}$$

$$B_5 = \frac{2A_2}{3} + \frac{A_5 + A_6}{6\mu_o}$$

$$B_6 = -\frac{2A_5}{\mu_o} \qquad (30a,b,c,d,e,f,g)$$

On rearrangement of Eq. (29), the quadratic form with variable dz becomes

$$q_1 dz^2 + q_2 dz + q_3 = 0 \qquad (31)$$

where

$$q_1 = B_3^2 + B_4^2 + B_6^2 - \frac{f(\zeta)^2}{k^2}$$

$$q_2 = 2(B_1 B_3 + B_2 B_4 + B_5 B_6)\, d\varepsilon_x + 2(B_2 B_3 + B_1 B_4 + B_5 B_6)\, d\varepsilon_\theta$$

$$q_3 = (B_1^2 + B_2^2 + B_5^2)\, d\varepsilon_x^2 + (B_1^2 + B_2^2 + B_5^2)\, d\varepsilon_\theta^2 \qquad (32a,b,c)$$

The increment of the intrinsic time scale dz is calculated to be

$$dz = \frac{-q_2 \pm \sqrt{q_2^2 - 4q_1 q_3}}{2q_1} \qquad (33)$$

By definition, the intrinsic time measure ζ in Eq. (12a) is invariably greater than or equal to zero. The expression of $d\zeta$ in Eq. (12b) is expected to generate two roots of the opposite sign or zero value. The material function, as shown in Eq. (14), invariably exceeds zero. Therefore, two roots of opposite sign or zero value are found in Eq. (33); the positive root is the desired one.

The differential increments $d\varepsilon_x$ and $d\varepsilon_\theta$ are considered here to be the input value. The parameters A_1, .., A_6, B_1, .., B_6, q_1, q_2 and q_3 are determined according to the known values of ζ, z, ε_x, ε_θ, ε_r, σ_x and σ_θ at the current state of loading. The increment of the intrinsic time scale dz is determined from Eq. (33). Consequently, the incremental quantities $d\zeta$, $d\varepsilon_r$, $d\sigma_x$ and $d\sigma_\theta$ are obtained from Eqs. (14), (24), (26) and (27), respectively. The loading process can be readily completed by repeatedly updating the values of ζ, z, ε_r, σ_x and σ_θ during the calculation.

3.3. Principle of virtual work

The principle of virtual work, which satisfies the equilibrium requirement, is given by

$$\int_v \sigma_{ij}\, \delta\varepsilon_{ij}\, dV = \delta W \qquad (34)$$

where V is the volume of the material of the tube section considered, and δW is the virtual work of the external loads. For the case of thin-walled tube subjected to pure bending, the quantity of δW is equal to zero since the curvature is prescribed. Eq. (34) is expressed for the incremental loading to be (Shaw and Kyriakides 1985)

$$\int_v (\sigma_{ij} + \dot{\sigma}_{ij})\, \delta\dot{\varepsilon}_{ij}\, dV = 2R \cdot \int_0^{\pi} \int_{-t/2}^{t/2} [\hat{\sigma}_x\, \delta\dot{\varepsilon}_x + \hat{\sigma}_\theta\, \delta\dot{\varepsilon}_\theta]\, dT\, d\theta = 0 \tag{35}$$

where $\hat{\sigma}_x = \sigma + \dot{\sigma}_x$ and $\hat{\sigma}_\theta = \sigma + \dot{\sigma}_\theta$ and ($\dot{}$) denotes the increment of ( ). The in-plane displacement v and w are assumed to be symmetrical and are approximated by the following expression (Shaw and Kyriakides 1985, Kyriakides and Shaw 1987):

$$v \cong R \sum_{n=2}^{N} b_n \sin n\theta, \quad w \cong R \sum_{n=0}^{N} a_n \cos n\theta \tag{37a,b}$$

where the number of terms N is chosen to ensure satisfactory convergence. Kyriakides and Shaw (1987) investigated the sensitivity of the moment-curvature and ovalization-curvature responses for monotonic pure bending to the number of expansion terms used in Eqs. (37a) and (37b). Those equations clearly indicate that N=4 or 6 is sufficient. By Substituting Eqs. (4)-(8), (37a) and (37b) into Eq. (35) or (36), a system of $2N+1$ non linear algebraic equations in terms of $\dot{a}_o$, $\dot{a}_1$,..., $\dot{a}_N$, $\dot{b}_2$, $\dot{b}_3$,..., $\dot{b}_N$, $\dot{\varepsilon}_x^0$ are determined. This system of equations is solved using the Newton-Raphson method. The iterative scheme contains nested iterations for the constitutive relations. Kyriakides and Shaw (1987) provide a more detailed derivation of the system of equations for the loading cases of thin-walled tube under pure bending.

4. Results and discussions

In this study, the viscoplastic response of thin-walled tube subjected to cyclic bending is investigated experimentally and theoretically. The specimen for the experiment is AISI 304

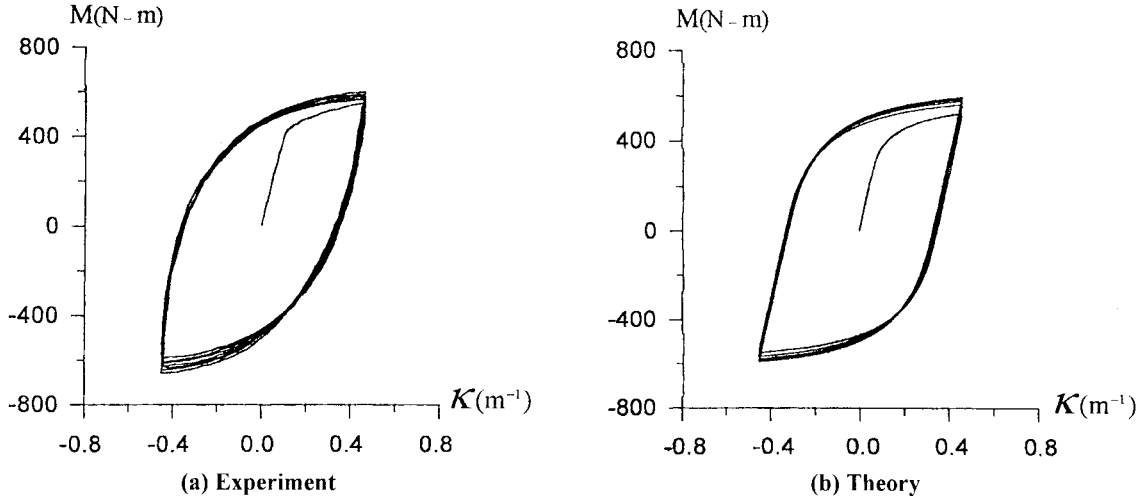

Fig. 8 Experimental and simulated moment-curvature curves at the curvature-rate of 2×10^{-3} m $^{-1}$/sec

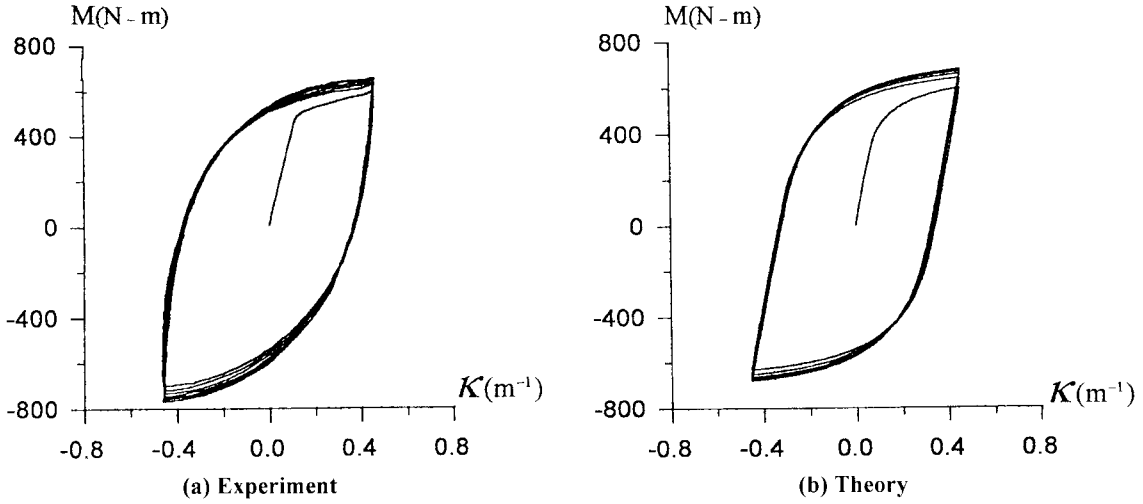

Fig. 9 Experimental and simulated moment-curvature curves at the curvature-rate of 2×10^{-1} m $^{-1}$/sec

stainless steel tube with outside diameter of 38.1 mm and wall thickness of 1.5 mm (D/t=25.4) and is cyclically bent under pure bending. The test is a curvature-controlled cyclic bending test with the curvature amplitude of ±0.5 m $^{-1}$. The curvature-rate is controlled by the COMA. The magnitudes of the curvature and the ovalization of the tube cross-section are measured by the COMA. Based on the capability of the bending machine, two maximum and minimum curvature-rates of 2×10^{-1} and 2×10^{-3} m $^{-1}$/sec are conducted to highlight the viscoplastic response of the thin-walled tube specimens under cyclic bending.

In the theoretical study, the kernel function of the endochronic theory is considered to compose by three terms of exponentially decaying function, therefore, the material parameters of the theory can be determined according to the method proposed by Fan (1983). The material parameters of the test material are determined to be: μ_o=5.91$\times10^4$ MPa, K=1.09$\times10^5$ MPa, C_1=7.0$\times10^5$ MPa,

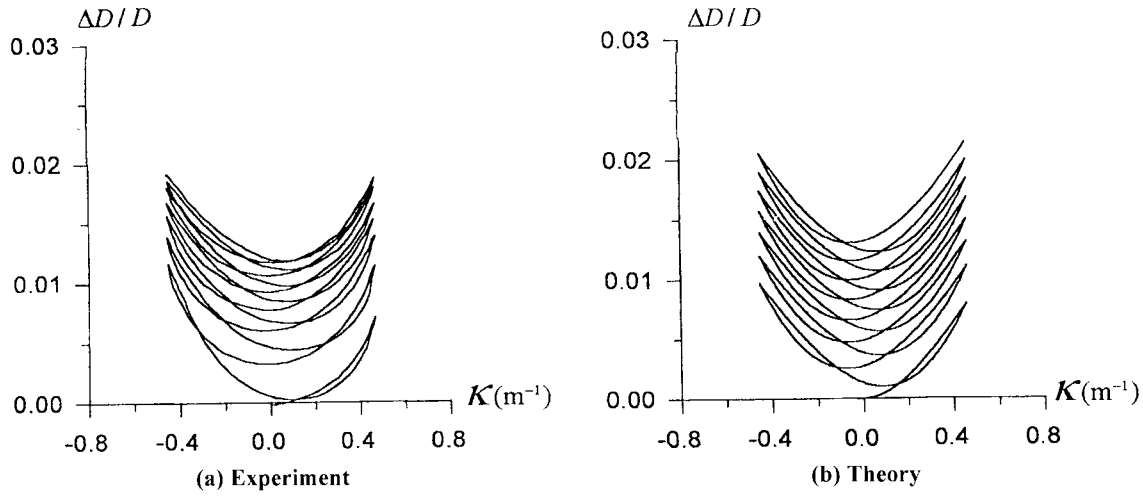

Fig. 10 Experimental and simulated ovalization-curvature curves at the curvature-rate of 2×10^{-3} m $^{-1}$/sec

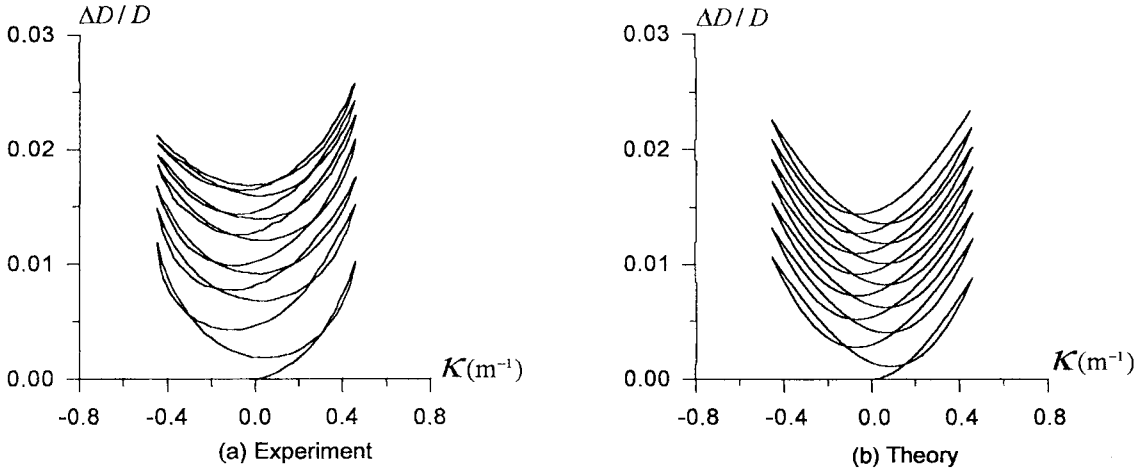

Fig. 11 Experimental and simulated ovalization-curvature curves at the curvature-rate of 2×10^{-1} m^{-1}/sec

α_1=9000, C_2=1.04×10^4 MPa, α_2=530, C_3=2.4×10^3 MPa, α_3=135, C=0.15, β=20, and k_a=0.05. Figs. 8(a) and 9(a) present the experimental results of cyclic moment-curvature curves for thin-walled tube specimen under the curvature-rates of 2×10^{-3} and 2×10^{-1} m^{-1}/sec, respectively. The magnitudes of moment at the curvature of 0.5 m^{-1} are 556 N-m for the first cycle and 603 N-m for the steady cycle under the curvature-rate of 2×10^{-3} m^{-1}/sec. However, the magnitudes of moment at the same curvature are 598 N-m for the first cycle and 648 N-m for the steady cycle under the curvature-rate of 2×10^{-1} m^{-1}/sec. It is shown that the moment-curvature curves are sensitive to the amount of the curvature-rate. The faster the curvature-rate implies, the faster degree of hardening for the tube specimen. Fig. 8(b) and 9(b) show the simulated results of the thin-walled tube under the curvature-rates of 2×10^{-3} and 2×10^{-1} m^{-1}/sec, respectively. Note that the simulated results are determined by using the theoretical formulation in Section 3. Figs. 10(a) and 11(a) present the experimental results of cyclic ovalization-curvature curves for thin-walled tube specimen under the curvature-rates of 2×10^{-3} and 2×10^{-1} m^{-1}/sec, respectively. It is shown that the ovalization-curvature curves are also sensitive to the amount of the curvature-rate and the ovalization of the tube cross-section increases when the curvature-rate increases. Fig. 10(b) and 11(b) show the corresponding simulated results for thin-walled tube specimen under the curvature-rates of 2×10^{-3} and 2×10^{-1} m^{-1}/sec, respectively. It is demonstrated that a reasonable correlation between the experimental and simulated results is achieved.

5. Conclusions

In this paper, the curvature-controlled experiments on thin-walled tubular specimens for AISI 304 stainless steel under cyclic bending at different curvature-rates are conducted to highlight the characteristic of viscoplastic response. The curvature-ovalization measurement apparatus (COMA), which was designed by Pan *et al.* (1998), is used for controlling the curvature-rate and measuring the magnitudes of the tube curvature and the ovalization of the tube cross-section. It is observed that the faster the curvature-rate implies, the fast degree of hardening of the metal tube. However, the ovalization of the tube cross-section increases when the curvature-rate increases.

In addition, the first-order differential constitutive equations of endochronic theory, which were

obtained by Murakami and Read (1989), with the rate-sensitivity function of the intrinsic time measure, which was proposed by Pan and Chern (1997), are used for investigating the viscoplastic response of thin-walled tube subjected to cyclic bending. A virtual work approach is used to formulate the problem, which results in a set of nonlinear algebraic equations that are numerically solved. It has been shown that the predictions correlate well with the experimental results.

Acknowledgements

The work presented was carried out with the support of National Science Council under grant NSC 85-2212-E-006-013. Its support is gratefully acknowledged.

References

Brazier, L.G. (1927), "On the flexure of thin cylindrical shells and other thin section", *Proceeding of the Royal Society*, Series A, **116**, 104-114.

Corona, E. and Kyriakides, S. (1988), "On the collapse of inelastic tubes under combined bending and pressure", *Int. J. Solids Struct.*, **24**(5), 505-535.

Fabian, O. (1981), "Elastic-plastic collapse of long tubes under combined bending, and pressure load", *Ocean Engng.*, **3**, 295-330.

Fan, J. (1983), "A comprehensive numerical study and experimental verification of endochronic plasticity", Ph.D. Dissertation, Department of Aerospace Engineering and Applied Mechanics, University of Cincinnati.

Gellin, S. (1980), "The plastic buckling of long cylindrical shell under pure bending", *Int. J. Solids Struct.*, **16**, 397-407.

Ikegami, K. and Ni-Itsu, Y. (1983), "Experimental evaluation of the interaction effect between plastic and creep deformation", *Plasticity Today Symposium*, Udine, Italy, June, 27-30.

Krempl, E. (1979), "An experimental study of room-temperature rate-sensitivity, creep and relaxation of AISI type 304 stainless steel", *J. Mech. Phy. Solids*, **27**, 363-375.

Kujawski, D. and Krempl, E. (1981), "The rate(time)-dependent behavior of Ti-7Al-2Cb-1Ta titanium alloy at room temperature under quasi-static monotonic and cyclic loading", *ASME J. Appl. Mech.*, **48**, 55-63.

Kyriakides, S. and Ju, G.T. (1992), "Bifurcation and localization instabilities in cylindrical shells under bending-I. experiments", *Int. J. Solids Struct.*, **29**(9), 1117-1142.

Kyriakides, S. and Ju, G.T. (1992), "Bifurcation and localization instabilities in cylindrical shells under bending-II predictions", *Int. J. Solids Struct.*, **29**(9), 1143-1171.

Kyriakides, S. and Shaw, P.K. (1982), "Response and stability of elastoplastic circular pipes under combined bending and external pressure", *Int. J. Solids Struct.*, **18**(11) 957-973.

Kyriakides, S. and Shaw, P.K. (1987), "Inelastic buckling of tubes under cyclic loads", *ASME J. Press. Vessel Technol.*, **109**, 169-178.

Murakami, H. and Read, H.E. (1989), "A second-order numerical scheme for integrating the endochronic plasticity equations", *Comput. Struct.*, **31**, 663-672.

Pan, W.F. and Chern, C.H. (1997), "Endochronic description for viscoplastic behavior of materials under multiaxial loading", *Int. J. Solids Struct.*, **34**(17), 2131-2160.

Pan, W.F., Lee, T.H. and Yeh, W.C. (1996), "Endochronic analysis for finite elasto-plastic deformation and application to metal tube under torsion and rectangular block under biaxial compression", *Int. J. Plasticity*, **12**(10), 1287-1316.

Pan, W.F., Wang, T.R. and Hsu, C.M. (1998), "A curvature-ovalization measurement apparatus for circular tubes under cyclic bending", *Experimental Mechanics*, **38**(2), 99-102.

Reddy, B.D. (1979), "An experimental study of the plastic buckling of circular cylinders in pure bending", *Int. J. Solids Struct.,* **15**, 669-683.

Reissner, E. and Weinitschke, H.J. (1963), "Finite pure bending of cylindrical tubes", *Q. Appl. Math.,* **20**, 305-319.

Shaw, P.K. and Kyriakides, S. (1985), "Inelastic analysis of thin-walled tubes under cyclic bending", *Int. J. Solids Struct.,* **21**(11), 1073-1100.

Valanis, K.C. (1980), "Fundamental consequence of a new intrinsic time measure-plasticity as a limit of the endochronic theory", *Archive Mechanics,* **32**, 171-191.